AD-A114 641 NAVAL RESEARCH LAB. WASHINGTON DC F/G 20/5
MAGNETO-OPTIC MATERIALS FOR BIASING RING LASER GYROS. REPORT 4,--ETC(U)
APR 82 G A PRINZ, J J KREBS, W G MAISCH
UNCLASSIFIED NRL-MR-4832 NL

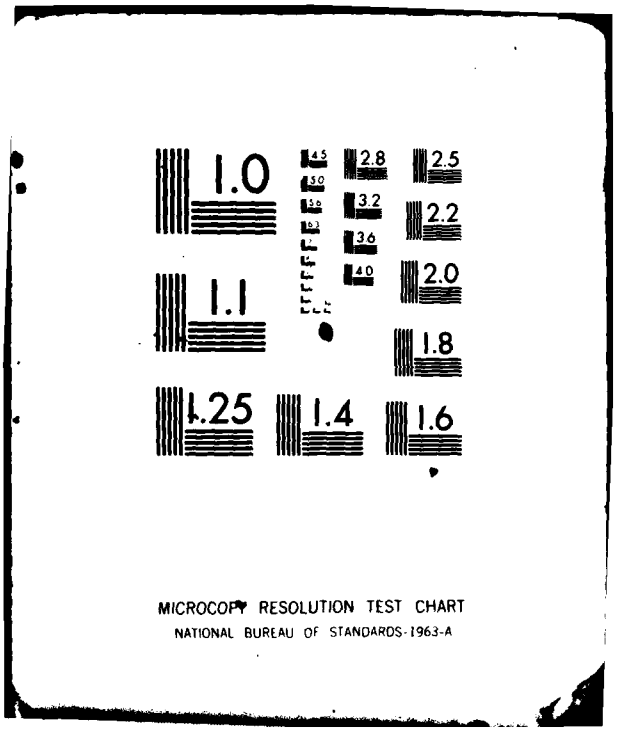
1.0
1.1
1.25
1.4
1.6
1.8
2.0
2.2
2.5
2.8
3.2
3.6
4.0
4.5
5.0
MICROCOPY RESOLUTION TEST CHART
NATIONAL BUREAU OF STANDARDS-1963-A

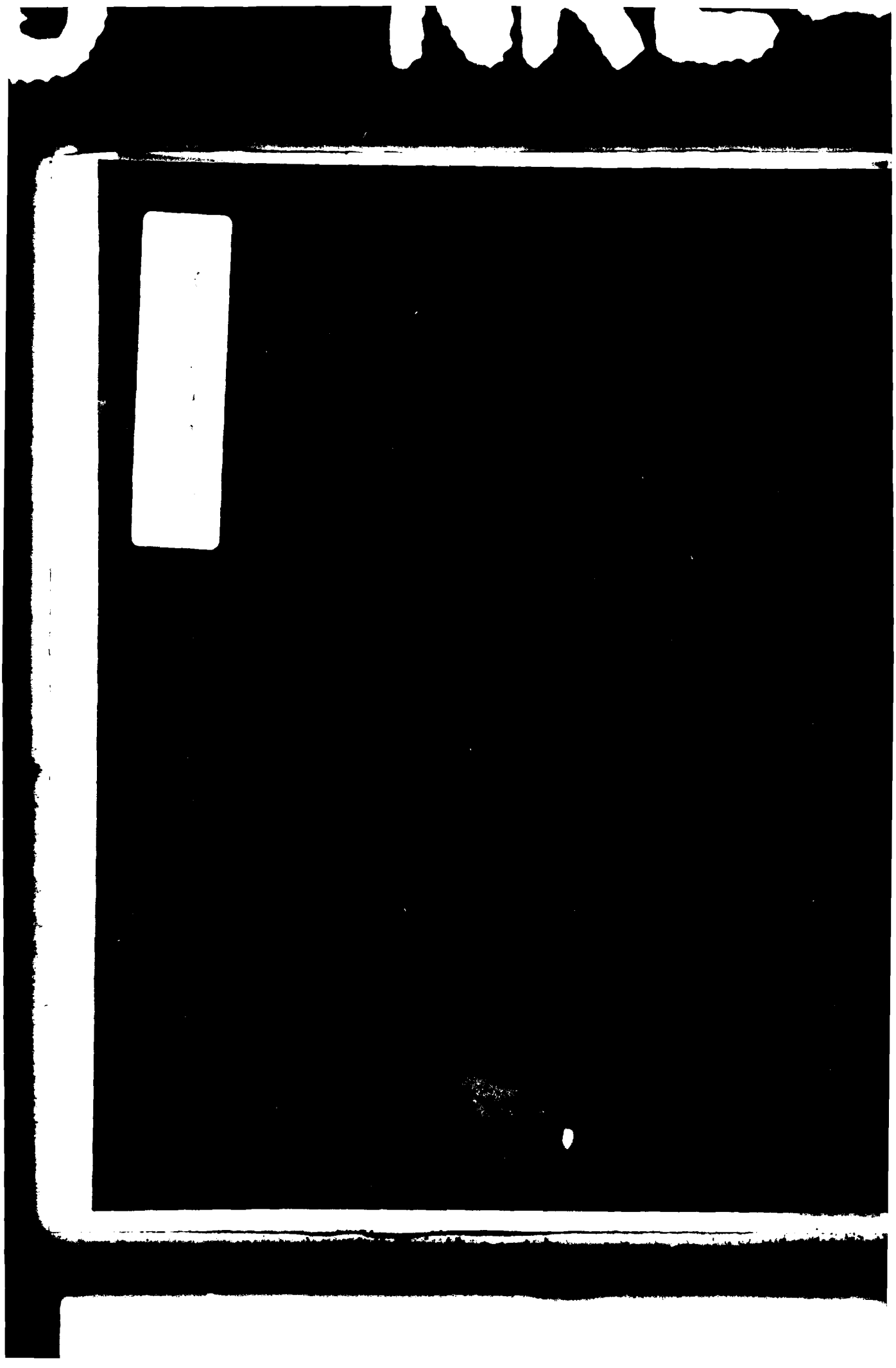

SECURITY CLASSIFICATION OF THIS PAGE (When Data Entered)

REPORT DOCUMENTATION PAGE	READ INSTRUCTIONS BEFORE COMPLETING FORM
1. REPORT NUMBER NRL Memorandum Report 4832	2. GOVT ACCESSION NO. AD-A114641	3. RECIPIENT'S CATALOG NUMBER
4. TITLE (and Subtitle) MAGNETO-OPTIC MATERIALS FOR BIASING RING LASER GYROS — REPORT NO. 4 — PROPERTIES OF EVAPORATED Fe-Co ALLOY FILMS		5. TYPE OF REPORT & PERIOD COVERED Interim report on a continuing NRL problem. 6. PERFORMING ORG. REPORT NUMBER
7. AUTHOR(s) G.A. Prinz, J.J. Krebs, W.G. Maisch and D.W. Forester		8. CONTRACT OR GRANT NUMBER(s)
9. PERFORMING ORGANIZATION NAME AND ADDRESS Naval Research Laboratory Washington, DC 20375		10. PROGRAM ELEMENT, PROJECT, TASK AREA & WORK UNIT NUMBERS 6272N; WF21-234 68-0821-0-2
11. CONTROLLING OFFICE NAME AND ADDRESS Department of the Navy Naval Air Systems Command Washington, DC 20361		12. REPORT DATE April 30, 1982 13. NUMBER OF PAGES 28
14. MONITORING AGENCY NAME & ADDRESS(if different from Controlling Office)		15. SECURITY CLASS. (of this report) UNCLASSIFIED 15a. DECLASSIFICATION/DOWNGRADING SCHEDULE

16. DISTRIBUTION STATEMENT (of this Report)

Approved for public release; distribution unlimited.

17. DISTRIBUTION STATEMENT (of the abstract entered in Block 20, if different from Report)

18. SUPPLEMENTARY NOTES

This program is supported by NAVAIRSYSCOM through ADPO-35 on Contract N00019-80-WR-01055.

19. KEY WORDS (Continue on reverse side if necessary and identify by block number)

LPS Vol 4
Laser gyros
Magneto-optical materials

20. ABSTRACT (Continue on reverse side if necessary and identify by block number)

The family of binary alloys $Fe_xCo_{(1-x)}$ for $1 \leq x \leq 0$ has been fabricated and characterized. Ellipsometric techniques are used to obtain the magneto-optical properties. Their performance as potential magneto-optical biasing elements is described.

DD FORM 1 JAN 73 1473 EDITION OF 1 NOV 65 IS OBSOLETE
S/N 0102-014-6601

SECURITY CLASSIFICATION OF THIS PAGE (When Data Entered)

CONTENTS

MAGNETO-OPTIC MATERIALS FOR BIASING RING LASER GYROS - REPORT No. 4
PROPERTIES OF EVAPORATED Fe-Co ALLOY FILMS

I. INTRODUCTION

This is the fourth of a series of reports on magneto-optical materials for biasing ring laser gyros. This report deals with the properties of the binary alloy system Fe_xCo_{1-x} for $1 \leq x \leq 0$. Previous reports in this series dealt with the magneto-optical properties of magnetic glasses (Report No. 1 - NRL Memorandum Report No. 3870) and of rare-earth: transition metal alloys (Report No. 2 - NRL Memorandum Report No. 4198). The Fe-Co alloy system appeared particularly attractive because it was known that some of the alloys exhibit larger magnetic moments than pure Fe. Magneto-optical effects generally scale with magnetic moment and since Fe exhibits the largest magneto-optical effects of all the elemental metals, it was expected that large effects would be observed in these alloys. Furthermore, the Fe-Co alloys are easily switched and possess very square hysteresis loops. These characteristics are specifically those sought for a magnetic mirror biasing element utilizing the transverse Kerr effect, of the type employed by Sperry Gyroscope Corporation in its laser gyroscope.

The magneto-optical properties of evaporated films of Fe-Co alloys have been studied in this work as a function of composition using ellipsometric techniques to obtain the components of the index of refraction $N = n-ik$ and the magneto-optical coefficient $Q = Q_1-iQ_2$ at the He-Ne laser wavelengths of $\lambda = 1.15\mu m$ and $0.63\mu m$. The results indicate a very sharply defined compositional range between $Fe_{.5}Co_{.5}$ and $Fe_{.6}Co_{.4}$ in which the atomic order-disorder transition affects the optical properties by increasing both n and k, as well as increasing $|Q|$ to values larger than any previously reported except for the compound MnBi.

II. BACKGROUND

It has long been known that elemental Fe and Co exhibit large magneto-optical effects and these properties have been studied in some detail[1]. It has also been known that alloys of Fe and Co can exhibit larger magnetization than either of the elemental constituents, as well as exhibiting an atomic order-disorder transition ($\approx 730°C$) for compositions near $Fe_{.5}Co_{.5}$. This transition is characterized by a rearrangement of the constituents of the bcc structure from having random locations in the disordered state to having one element only on cube corners and the other element only at cube centers in the ordered state. [The optical properties of these alloys have not, however, until recently been investigated.] The recent work of Kudryavtsev et al[2]

Manuscript submitted March 23, 1982.

indicated that for $Fe_{.5}Co_{.5}$ dramatic changes occur in the optical conductivity when thin-film samples are annealed and presumably pass through the order-disorder transition. These effects were interpreted on the basis of changes in the band structure when the system formed an ordered superlattice[3] structure.

III. EXPERIMENTAL

a) Procedures

Polycrystalline films were prepared by co-evaporation of the constituents from two separate e-beam sources in a vacuum of 10^{-7} Torr onto optically polished fused quartz substrates. The substrates were heated via thermal contact with a copper plate whose temperature was monitored with a thermocouple. Substrate temperatures (T_a) of up to 400°C were utilized to anneal the films during growth. The samples were approximately 3000 Å thick and of good optical quality.

The transverse Kerr effect was used to measure the complex magneto-optical coefficient $Q \equiv (Q_1 - iQ_2)$ at room temperature and at the wavelengths of the He-Ne laser $\lambda = 0.63\ \mu m$ (2.0eV) and $\lambda = 1.15\ \mu m$ (1.1eV). The quantity Q is defined in terms of the off-diagonal component of the dielectric tensor of the material as follows:

$$= \varepsilon_o \begin{pmatrix} N^2 & -iQN^2 & 0 \\ iQN^2 & N^2 & 0 \\ 0 & 0 & N^2 \end{pmatrix}. \qquad (1)$$

where N is the complex index of refraction ($N \equiv n-ik$), ε_o is the dielectric constant of free space and the magnetization M is assumed to be along z. Since one requires all four quantities n, k, Q_1, and Q_2 in order to evaluate the magneto-optical effects for a metallic mirror, an ellipsometric technique was used to make the measurements.

The experimental apparatus shown in Fig. 1 permits one to determine all of the required parameters by taking data both with and without an applied magnetic field H. The sample holder electromagnet produces a DC field up to 120 Oe in the plane of the film and normal to the plane of incidence. In order to eliminate the (rather severe) effects of thin surface oxide layers, data were taken through the fused quartz substrate using the fused quartz prism shown in Fig. 1 together with an index matching fluid. We used a measurement technique similar to that developed by Robinson[4] for longitudinal Kerr effect work. However, redundant data were used to cancel systematic errors. Because of growth induced anisotropy in the films, the easy axis was

first determined and all data was taken with that axis along the applied field. All samples were measured in a saturated state.

The easy axis was determined from hysteresis curves of M vs H measured on the samples using an M-H looper of the type described by Copeland[5]. The maximum drive field amplitude was 70 Oe at 100 Hz. The saturation magnetization per unit volume, M_s, was obtained from a vibrating coil magnetometer measurement on an identical sample. More details on the experimental methods can be found in Report No. 1.

b) Results

The results of these measurements are presented in Figs. 2, 3, 4, 5, and 6. The bulk of the data presented is for samples which were annealed to 250°C. Limitations on our apparatus prohibited us from preparing many samples at a higher T_a within a reasonable time. Some samples were prepared at 400°C however, and that data is included. The figures all present the data in terms of increasing Co concentration and the bulk change of phase from body-centered-cubic to face-centered-cubic at $Fe_{.25}Co_{.75}$ is indicated. This often coincides with a break in the behavior of the data. In general, the quality of the visible data at λ = 0.63 μm (2.0eV) is higher than the infrared data at λ = 1.15 μm (1.1eV). This stems from the fact that accurate ellipsometry is dependent upon precise determination of a null signal through the instrument. The much poorer signal-to-noise obtained from the infrared source and detector made these nulls less certain. The lines drawn in the figures connecting the data points are merely intended to aid the eye.

Figure 2 shows n and k vs composition for λ = 0.63 μm, and the most notable fact is the sharp increase in both quantities in the compositional range ≈ 40% Co to 50% Co. Two points for a $Fe_{.5}Co_{.5}$ sample annealed at 400°C are included.

Figure 3 illustrates the conductivity σ, calculated from n and k for both laser wavelengths. This quantity is often more popular in the literature, especially in calculations derived from band theory, and is therefore provided to facilitate comparisons.

Figure 4 contains the real and imaginary components of the magneto-optical tensor, Q_1 and Q_2 respectively, for λ = 0.63 μm (2.0eV). The maxima associated with the 40% Co to 50% Co region are less dramatic, but nevertheless quite apparent.

Figure 5 displays |Q| for both wavelengths. This quantity is generally the most important parameter from an applications point-of-view since it measures the magnitude of observed magneto-optic effects. Although the infrared data changes more gradually with composition than the visible data, it nevertheless shows large increases in the magneto-optic effects near $Fe_{.5}Co_{.5}$, since values of |Q| approaching 0.1 have never before been reported for transition metal alloys, and only exceeded by values reported for MnBi.

Finally, Fig. 6 exhibits the dependence of the 2.0eV value of |Q| divided by the saturation magnetization M_s for each composition. The behavior of

this ratio illustrates that the popular view of $|Q|$ being proportional to M_s is a misconception. The dramatic increase in $|Q|/M_s$ ($\approx 50\%$ at $Fe_{.5}Co_{.5}$) indicates that the magneto-optical properties of 2.0eV are far more sensitive to the ordering phenomena than is the magnetization.

IV. MAGNETO-OPTIC MIRROR APPLICATION

The principal interest in these magnetic alloys, from the point-of-view of this report, lies in their potential application as magneto-optic biasing elements in a ring laser gyro. In particular, they would be employed as transverse Kerr effect mirrors, in essentially the same configuration illustrated in. Fig. 7. In order to predict the behavior of such mirrors a computer model was developed which generated the performance figures for any arbitrary element design. This computer program was the subject of Report No. 3 in this series. For the purposes of this present Report we employed the program to generate graphical respresentations of: a) The reflectivity of p-polarized radiation R; b) the differential reflectivity ΔR; c) the differential phase shift $\Delta\Phi$; and d) the figure-of-merit (FM). The quantities are defined respectively as follows:

$$R = \frac{1}{2}(|R_{pp}(Q) + R_{pp}(-Q)|^2) \tag{2}$$

$$\Delta R = (|R_{pp}(Q)|^2 - |R_{pp}(-Q)|^2)/R \tag{3}$$

$$\Delta\Phi = \text{Arg}\{R_{pp}(Q)\} - \text{Arg}\{R_{pp}(-Q)\} \tag{4}$$

$$FM = \Delta\Phi/(1-R) \tag{5}$$

where Arg {X} means the argument of the complex quantity X and R_{pp} is the Fresnel reflection coefficient. More detail can be found in Report No. 3[6].

The optical structure chosen is illustrated in Fig. 8. It contains six pairs of dielectric layers (high-low index) tuned to enhance the reflectivity at the wavelength of interest and a 30° angle of incidence. The dielectric layer closest to the metal film is "tuned" in the usual manner to optimize the performance[6]. The calculations were performed for each of the He-Ne laser wavelengths of interest (0.63 μm and 1.15 μm) for several selected alloy compositions. The results are presented as Figs. 9 through 14, where in every case the performance is plotted as a function of tuning layer thickness in order to illustrate optimization. Finally in Fig. 15 the peak FM for the whole family of alloys is presented as a function of composition, again for the two wavelengths of interest.

V. DISCUSSION

There are several interesting implications of the above results, both in terms of physics and potential applications. First, it is apparent by inspection of the figures that the manifestations of the order-disorder transition

are not centered symmetrically about $Fe_{.5}Co_{.5}$, but are in fact centered at approximately $Fe_{.55}Co_{.45}$. This is an unexplained result which has also been seen in neutron-powder diffraction experiments on these alloys[7]. A simple Ising model description of the order-disorder transition predicts symmetry about $Fe_{.5}Co_{.5}$[8].

Another interesting physics question arises from the dramatic changes in the optical properties upon ordering. The 2eV optical conductivity σ increases 50% over the baseline values outside of the ordering region of composition. Evidence of this was first reported by Kudryavtsev et al who studied the spectral dependence of the optical conductivity in $Fe_{.5}Co_{.5}$ under different conditions of annealing. At the points where our two studies intersect (i.e. T_a = 250°C; $Fe_{.5}Co_{.5}$; E = 1.1eV and 2.0eV) our results for σ are in good agreement. They cite the band theory calculations of Yamashita et al[3] on the Fe-Co ordered superlattice for an explanation. Yamashita et al have shown that the principal effect of the ordering is to split certain bands at high symmetry points in the Brillouin zone, with a corresponding change in the wave functions. Kudryavtsev et al suggest that the optical conductivity at 2.0eV arises principally from the region around one of these points (P in the disordered structure which becomes R in the ordered structure). A neighboring transition at 1.4eV is attributed to the region around Γ where no band splitting occurs, hence the transition remains unaltered. This assignment for the source of the optical activity does not disagree with Singh et al[8] who have done a detailed band calculation of the optical properties of Fe. Singh et al also calculated the magneto-optical properties and determined that they arise chiefly from transitions about another high symmetry point N which becomes M in the ordered region and also undergoes splitting. It therefore appears as if the dramatic changes in the magneto-optical properties can be understood on this basis. While the spectral dependence of Q_1 and Q_2 has been measured in Fe and Co, no such study of $Fe_{.5}Co_{.5}$ has been reported which would locate specific spectral features that could be related to the band picture. It should be noted that while the quantities n, k, Q_1, and Q_2 are sensitive to the detailed behavior of the energy bands and wave functions at certain points in the Brillouin zone, the magnetization depends only upon the projected density of states for up and down spins near the Fermi level, which changes very little upon ordering[3]. While this makes the data of Fig. 6 easier to understand it must be remembered that the magneto-optical effects arise entirely from the spin-orbit interaction and its proper inclusion in band calculations has been attempted only recently[9]. Results are not yet available for the superlattice FeCo.

Finally, from an applications point of view, it appears as if the Fe-Co alloy system can provide materials of much greater magneto-optical activity than one might have expected from the well known 10% increase in M_s for $Fe_{.7}Co_{.3}$ over Fe. The values of $|Q|$ reported for the ordered region are considerably higher than had been previously known for magnetically switchable materials. Since the saturation annealing temperature of 350°C found by Kudryavtsev et al was not reached for the bulk of the samples in this study,

they did not reflect the properties of samples possessing complete long-range order. The larger values of n, k, Q_1, and Q_2 suggested by our 400°C data might reasonably be expected to be obtained. Furthermore, in the ordered state these are easily-switched, very square hysteresis loop materials, which is often an important property for applications.

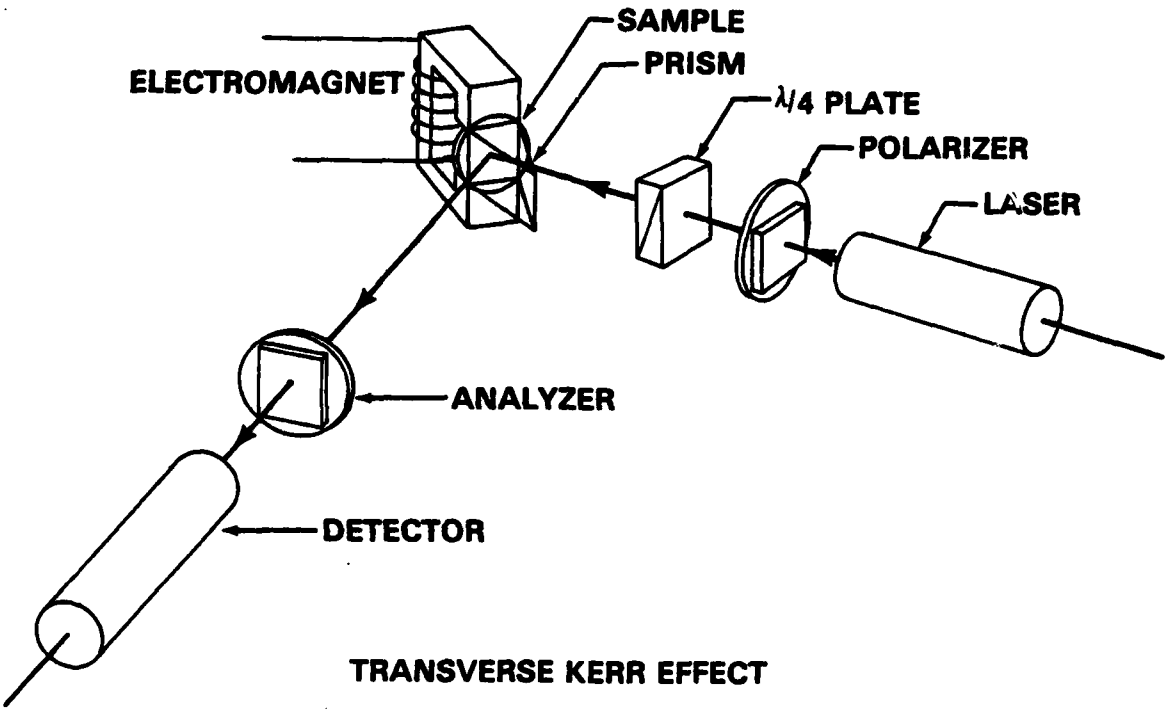

Figure 1

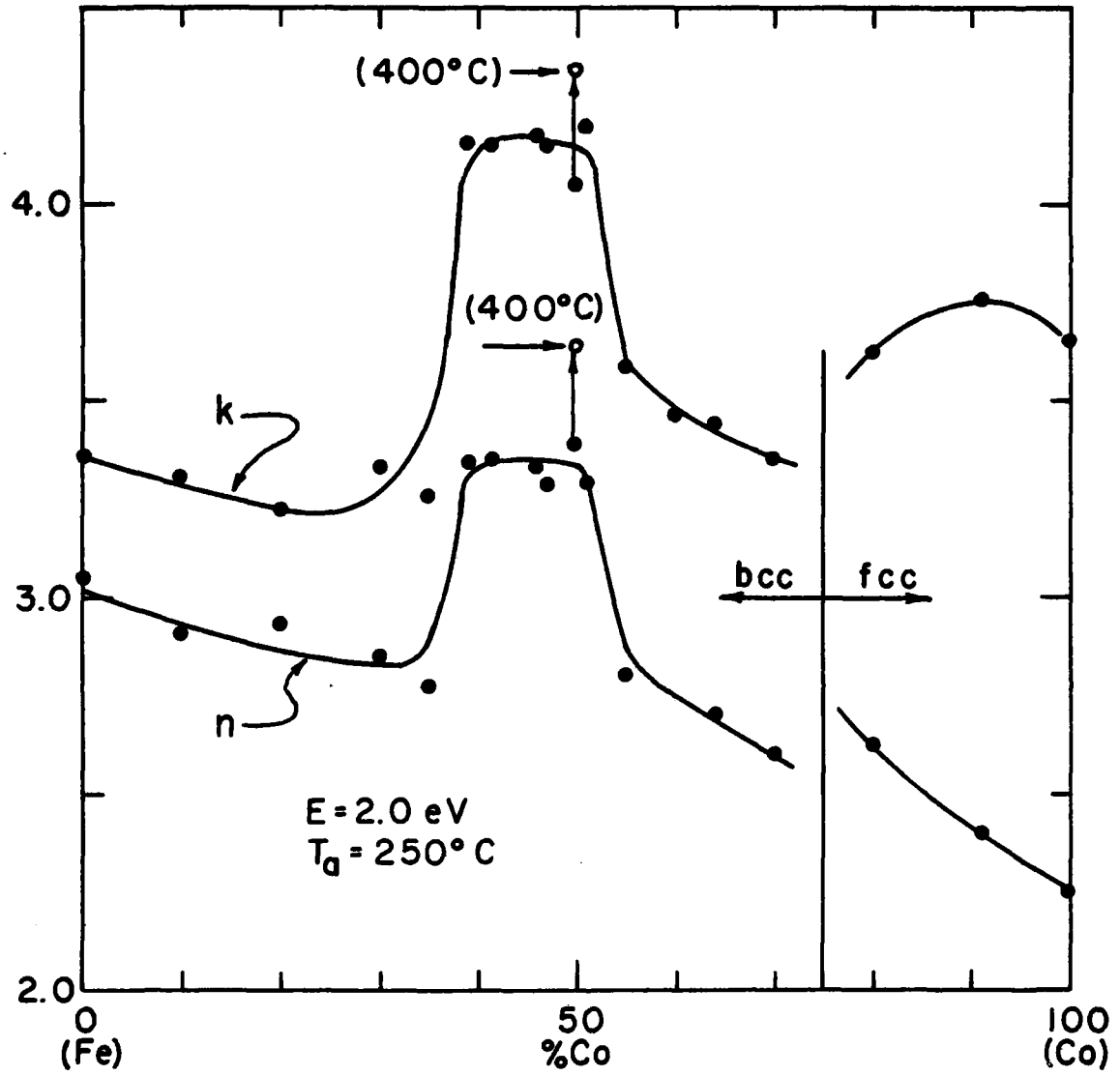

Fig. 2 — Real (n) and imaginary (k) components of the optical index vs. composition

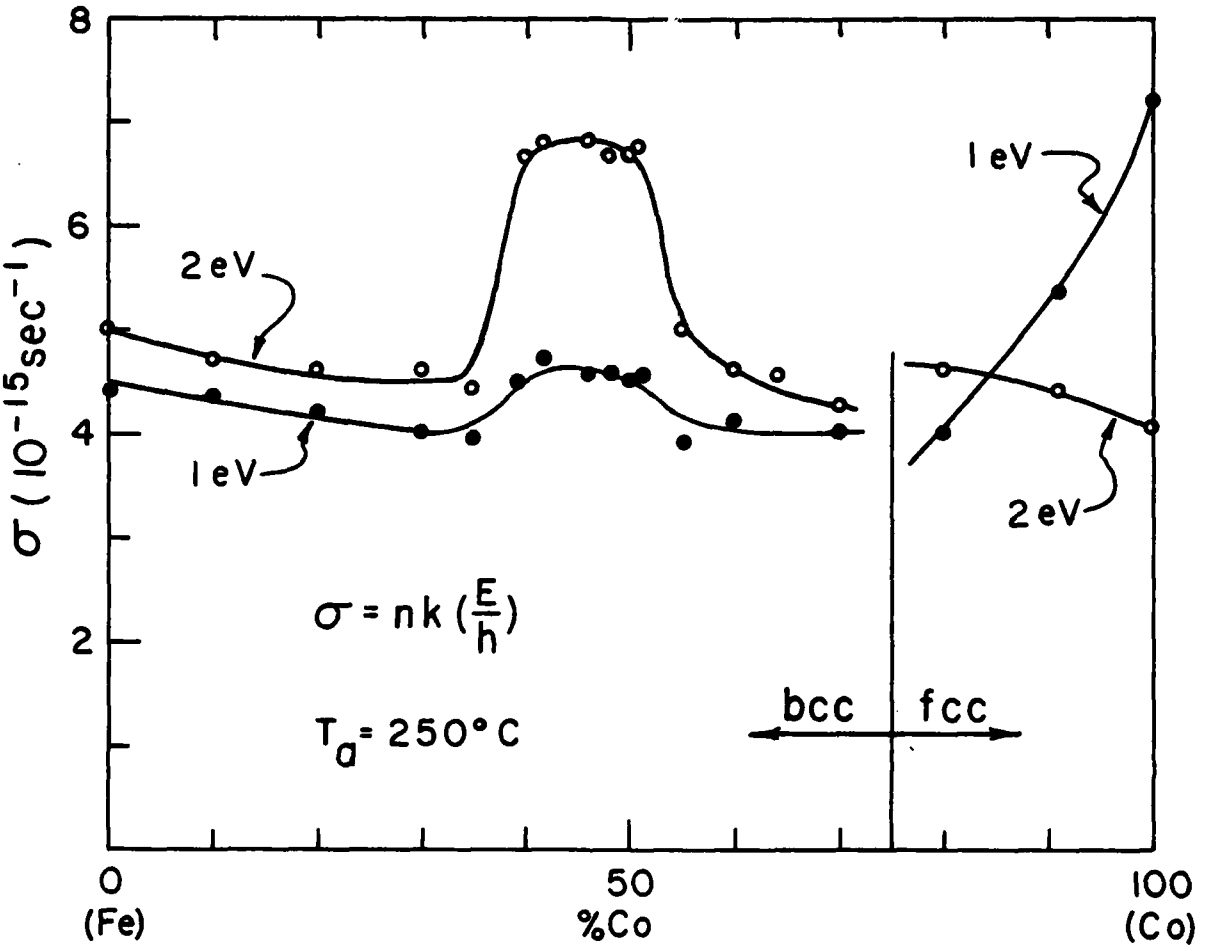

Fig. 3 — Optical conductivity (σ) vs. composition

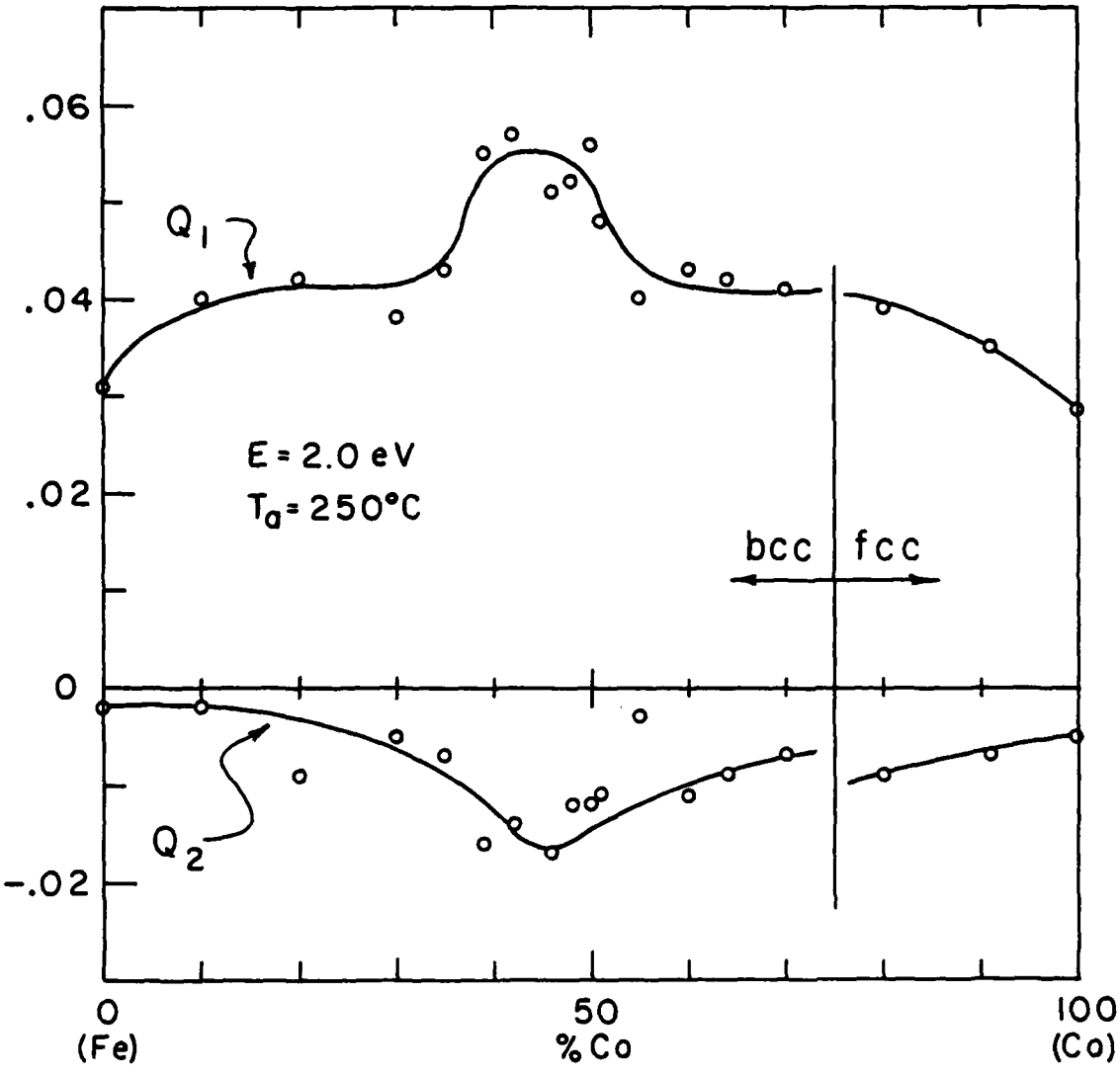

Fig. 4 — Real (Q_1) and imaginary (Q_2) components of the magneto-optical coefficient vs. composition

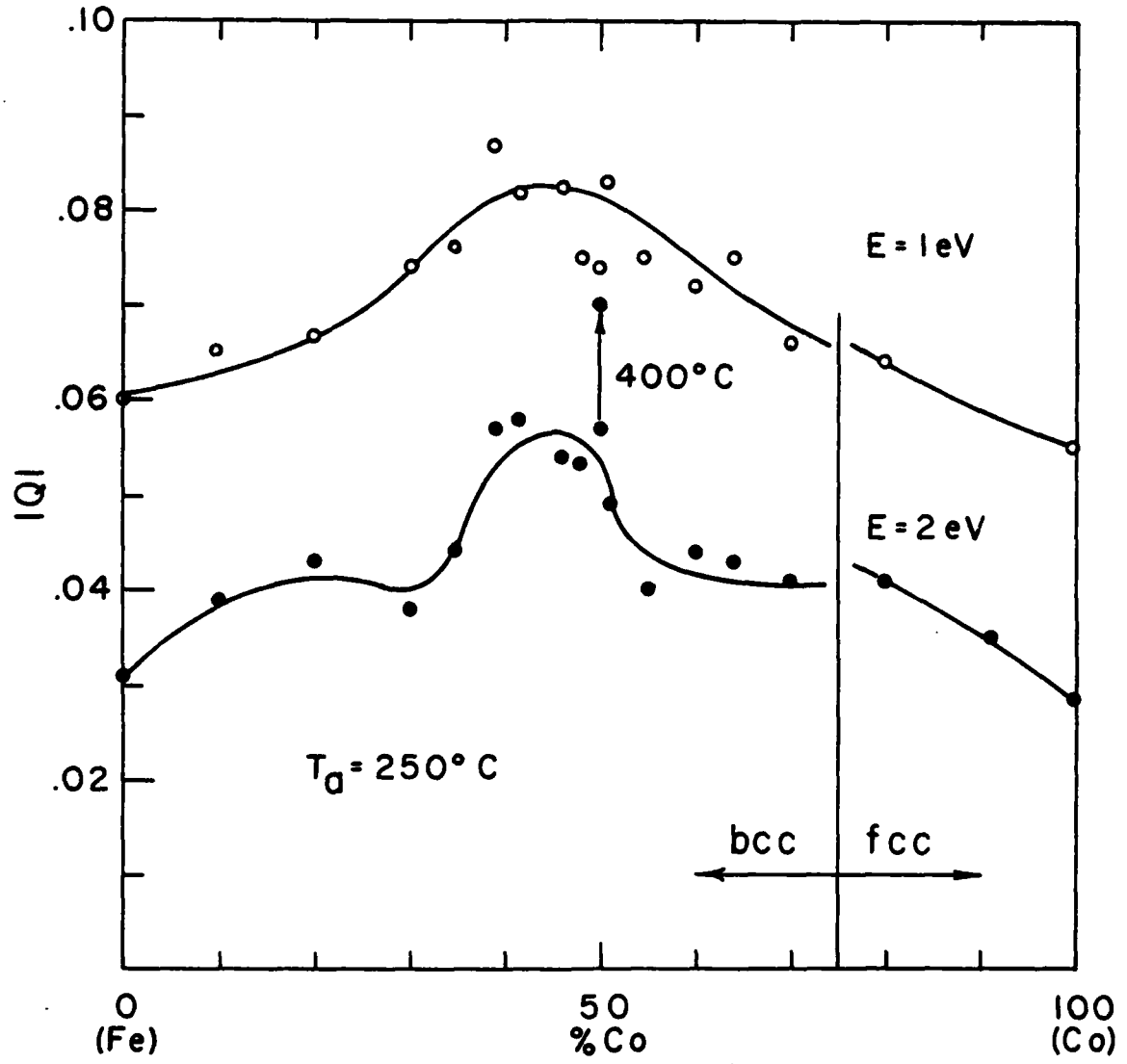

Fig. 5 — Absolute value of the magneto-optical coefficient vs. composition

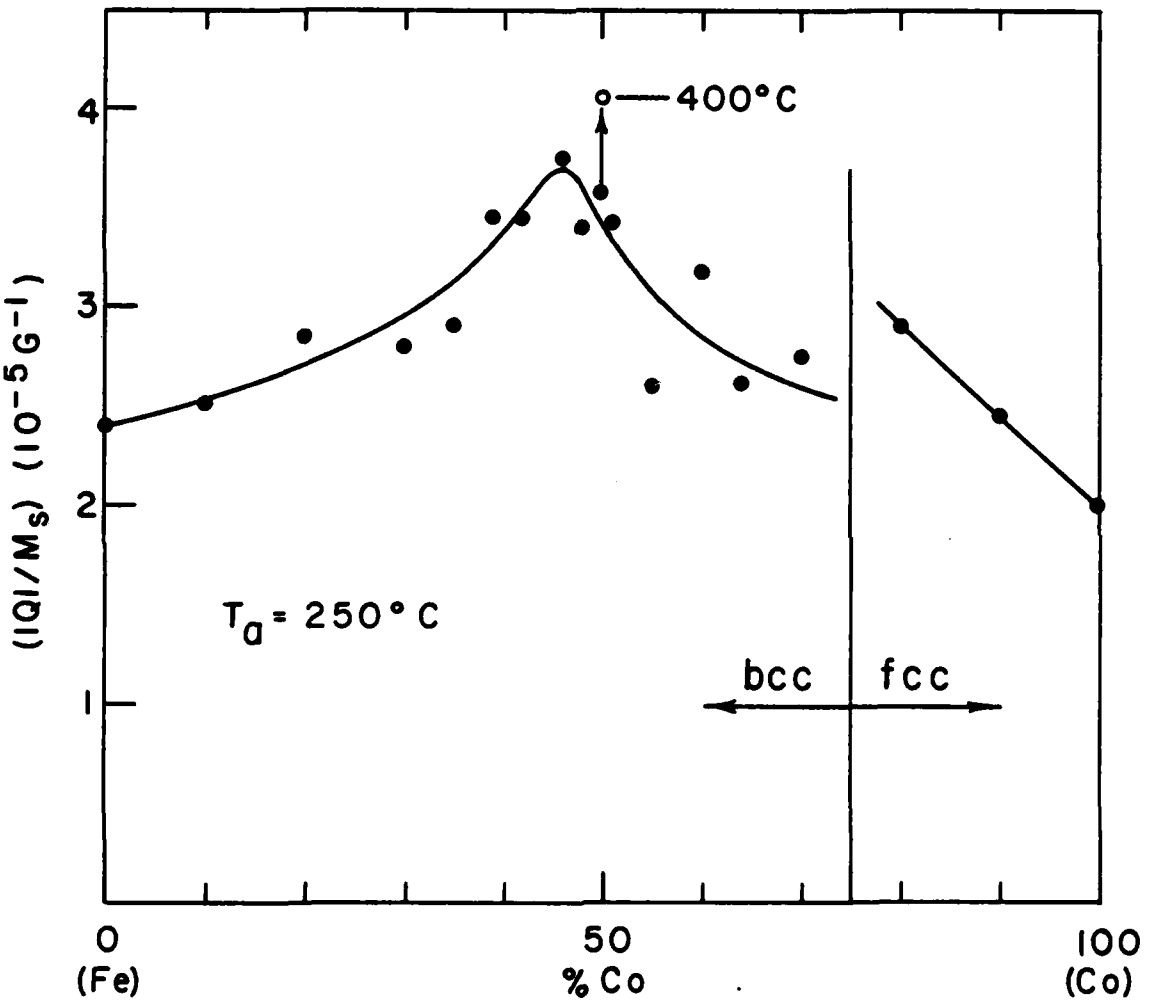

Fig. 3 — Ratio of the absolute value of the magneto-optical coefficient divided by the saturation magnetization vs. composition at λ = 0.63μm (2.0 eV)

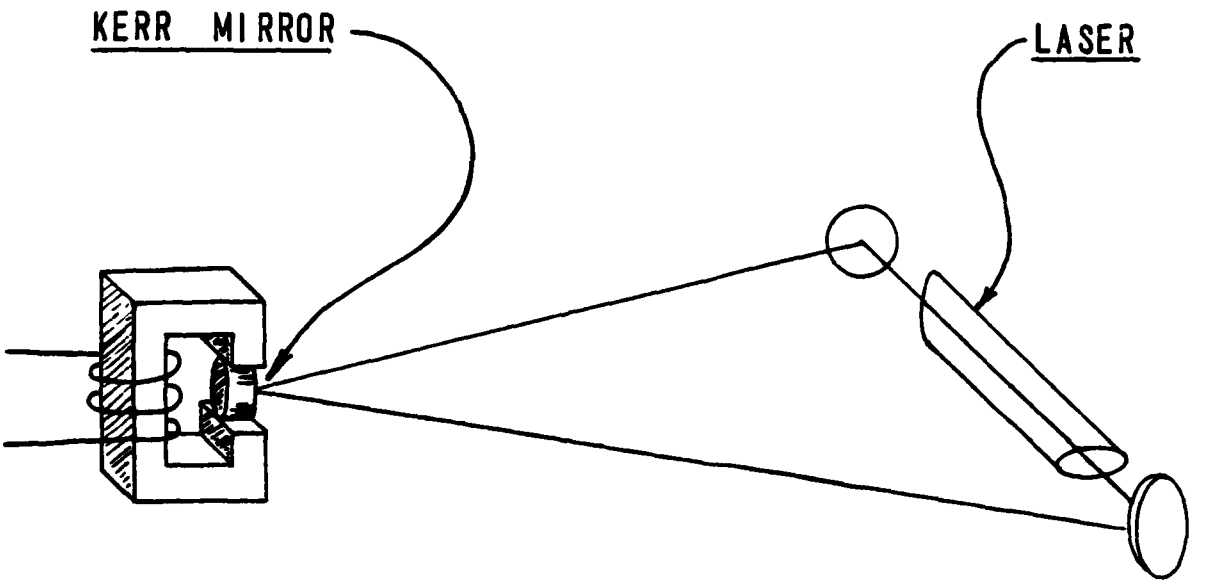

Fig. 7 — Laser gyro configuration employing transverse Kerr effect mirrors for magneto-optic biasing

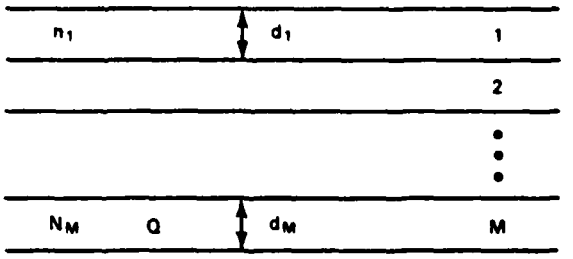

Fig. 8 — Optical structure used for computer model calculation

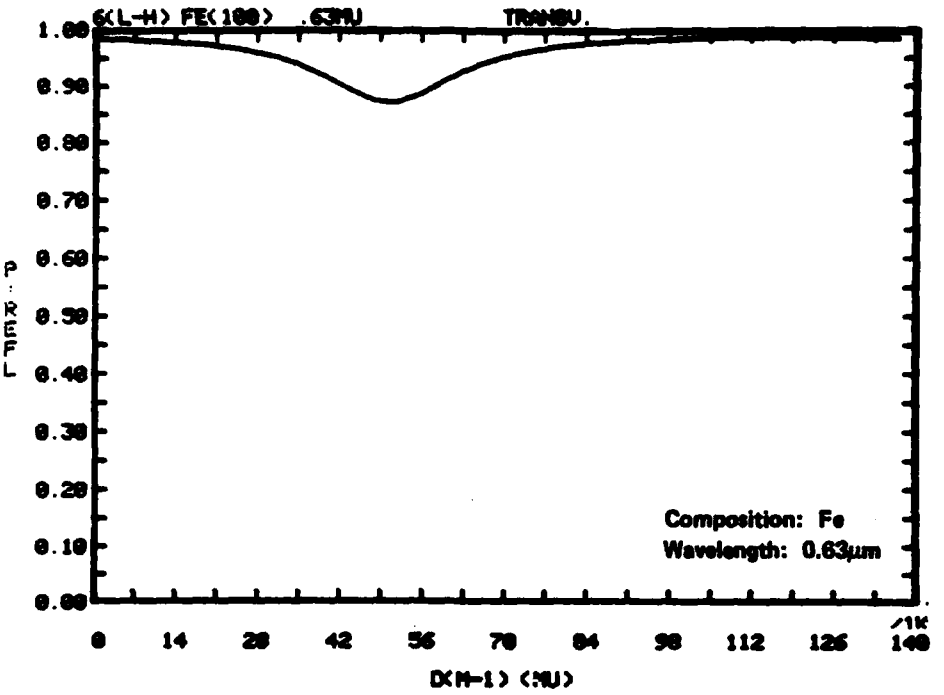

Fig. 9(a) — R vs tuning

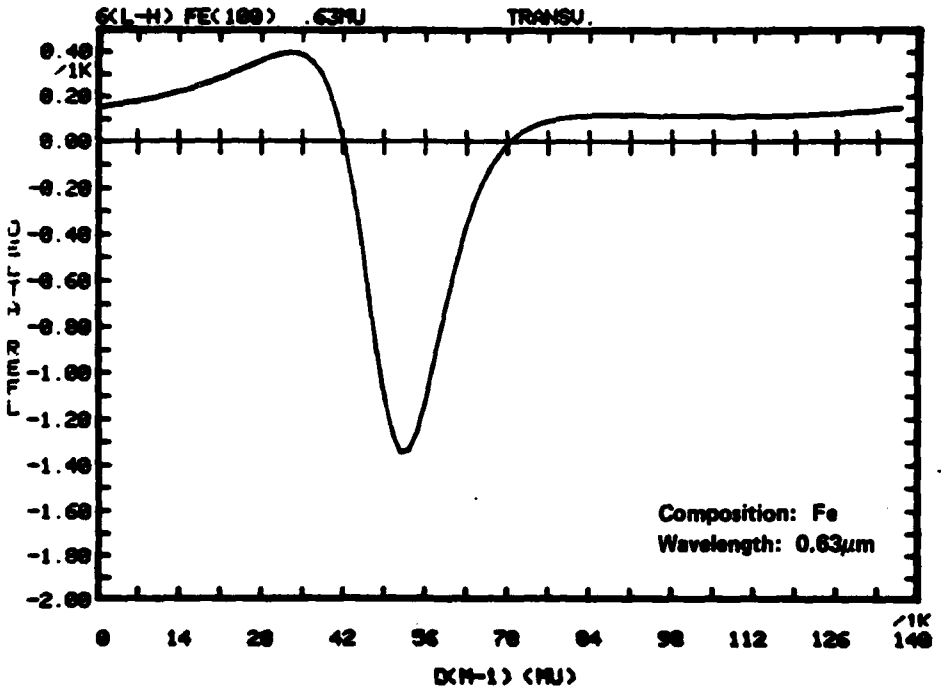

Fig. 9(b) — ΔR vs tuning

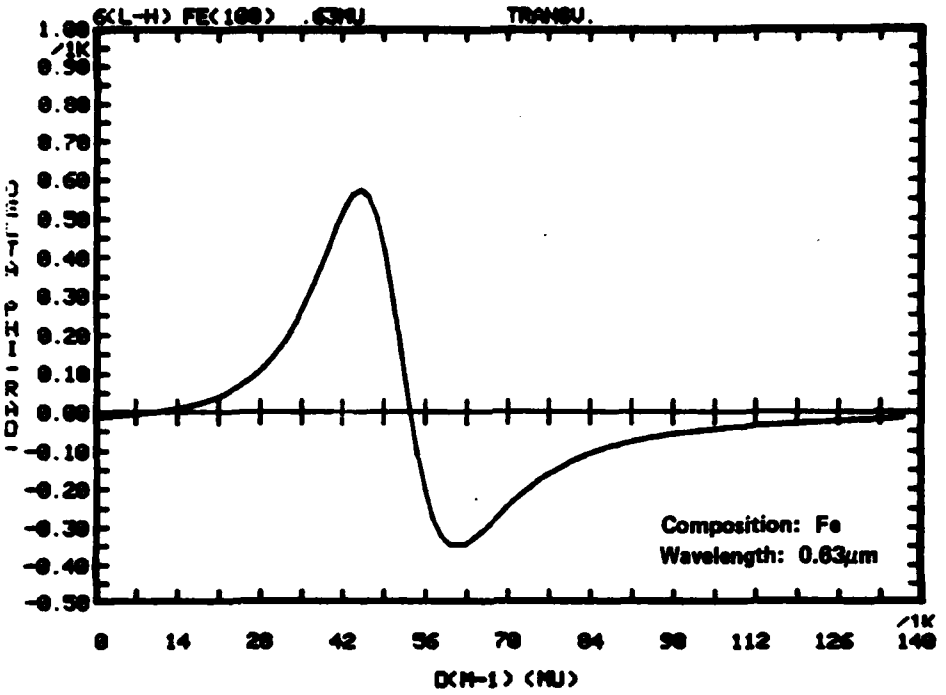

Fig. 9(c) — $\Delta\Phi$ vs tuning

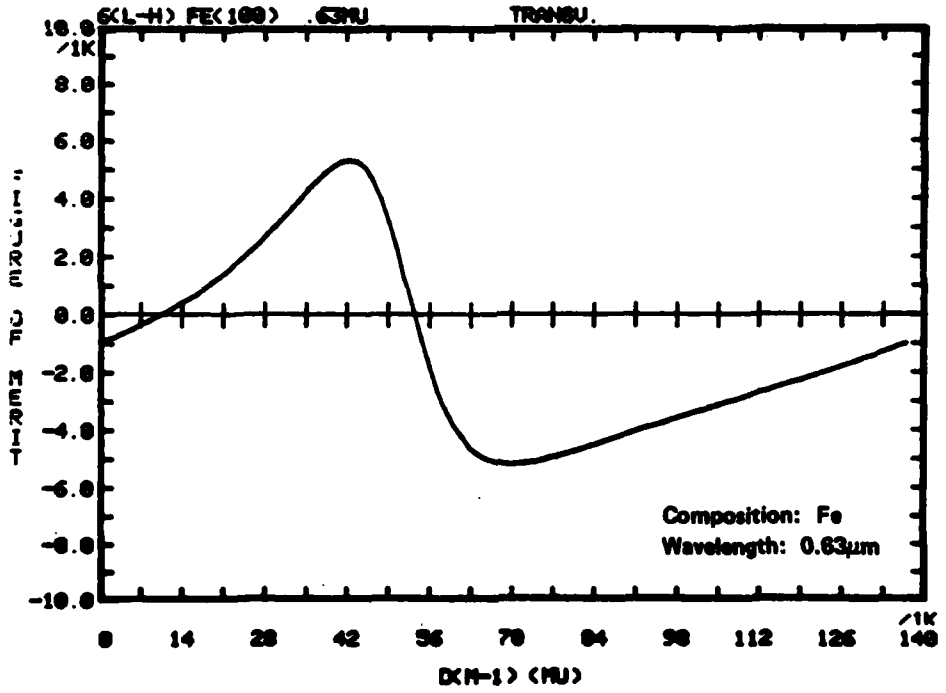

Fig. 9(d) — FM vs tuning

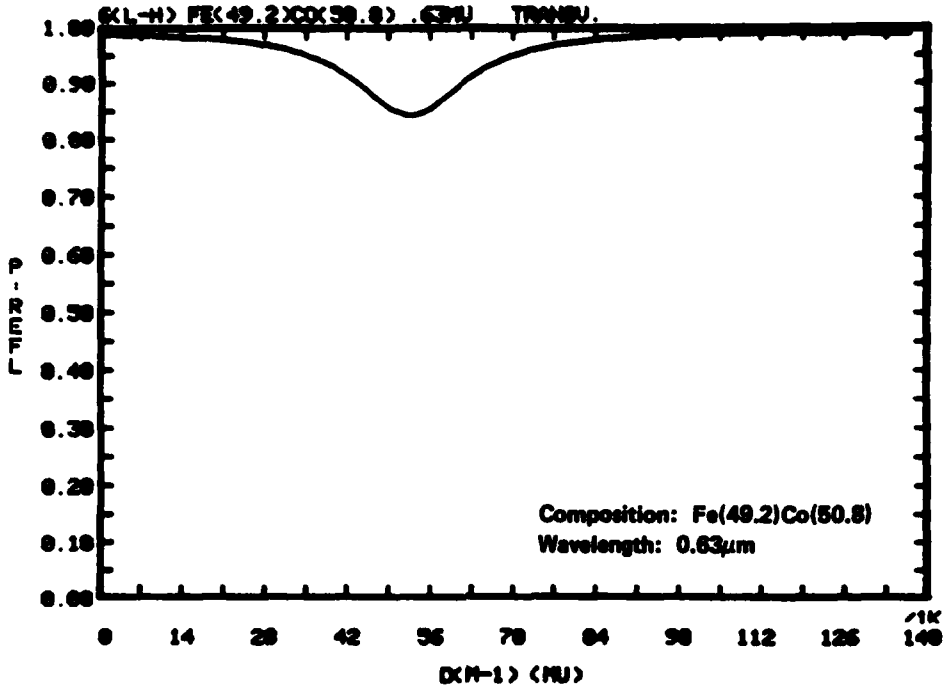

Fig. 10(a) — R vs tuning

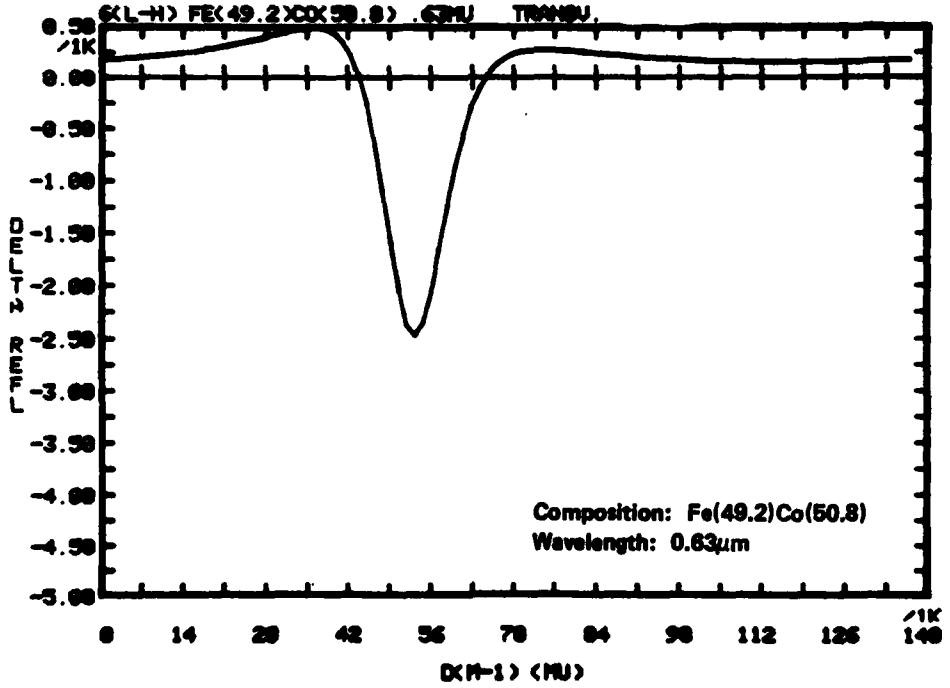

Fig. 10(b) — ΔR vs tuning

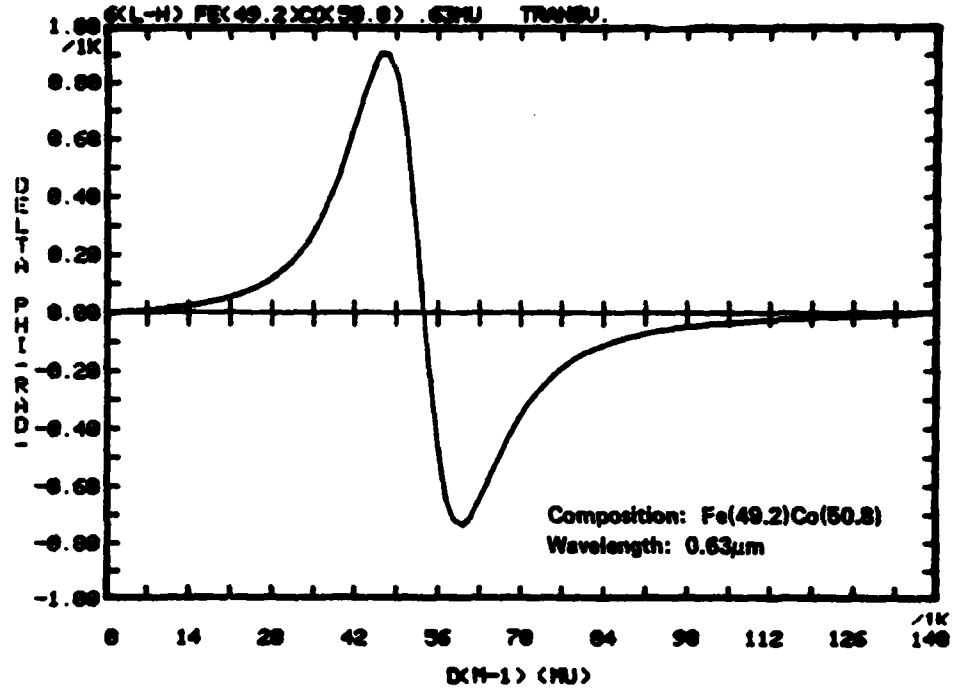

Fig. 10(c) — $\Delta\Phi$ vs tuning

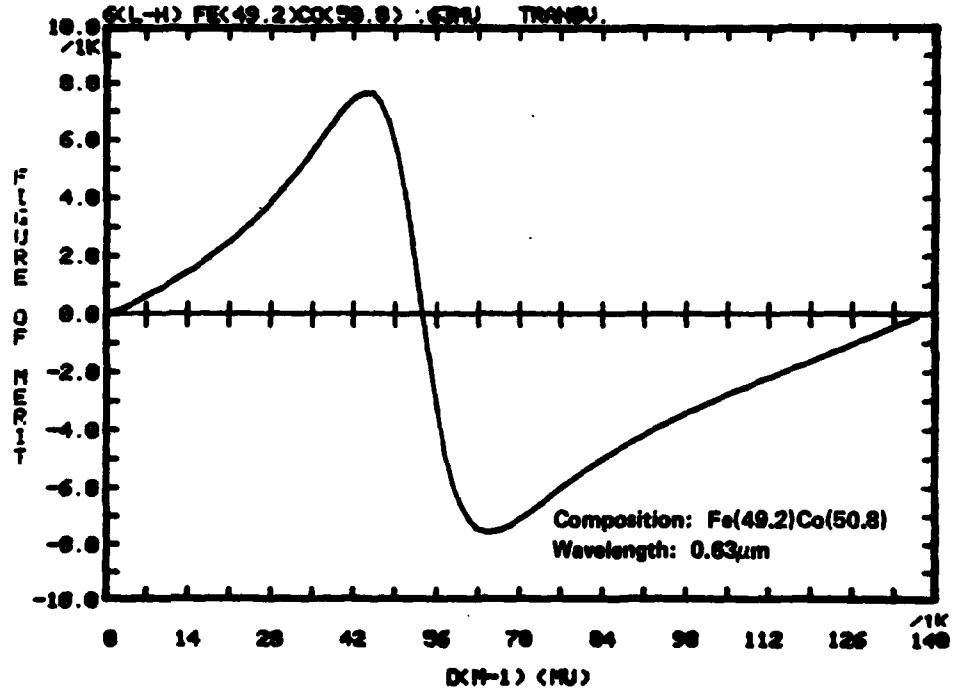

Fig. 10(d) — FM vs tuning

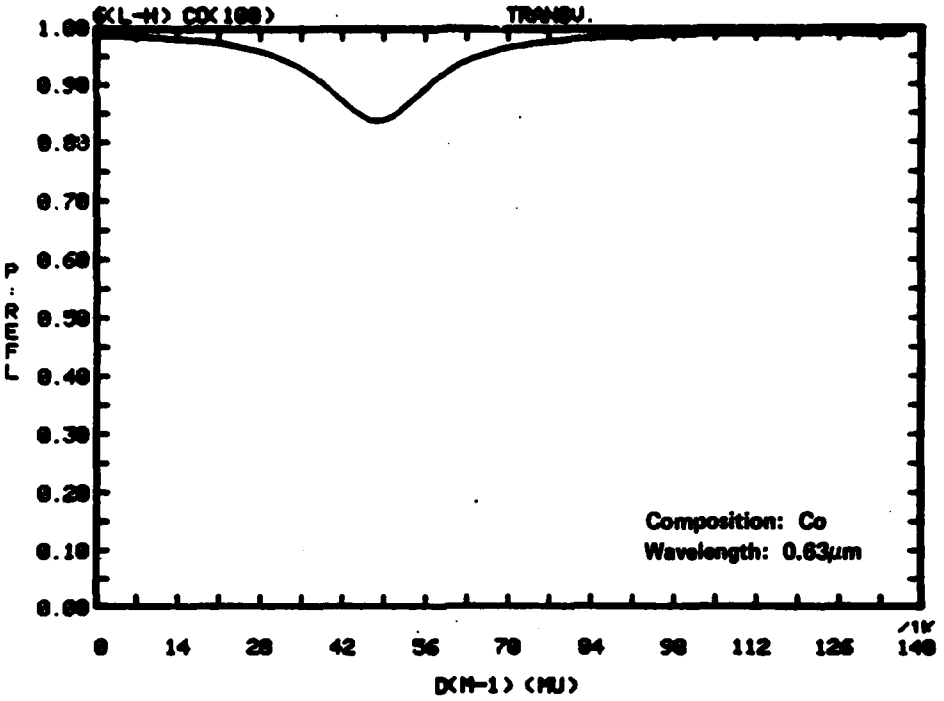

Fig. 11(a) — R vs tuning

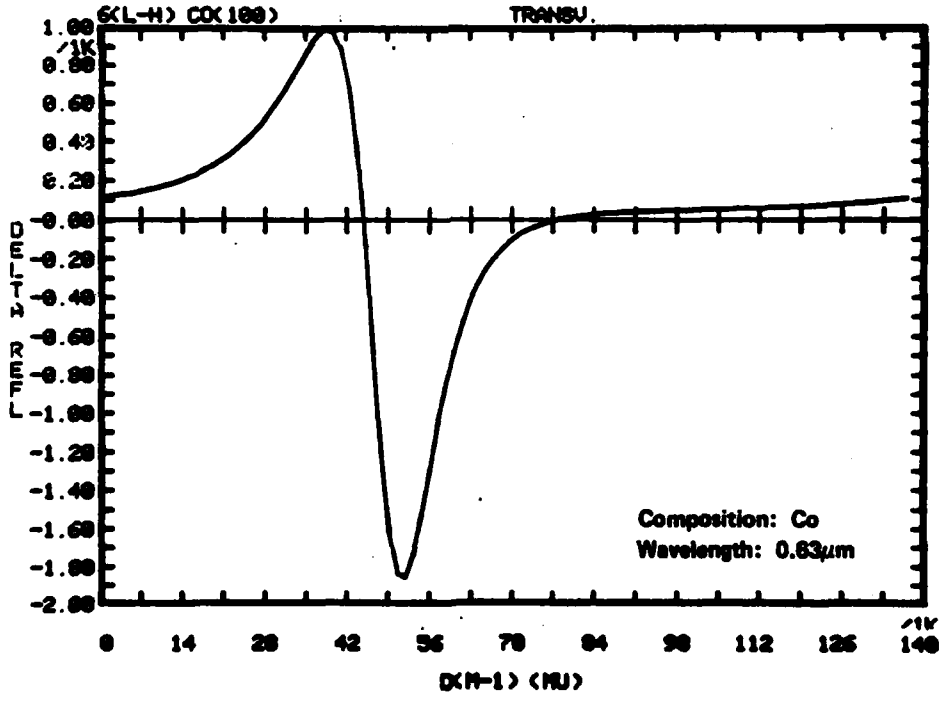

Fig. 11(b) — ΔR vs tuning

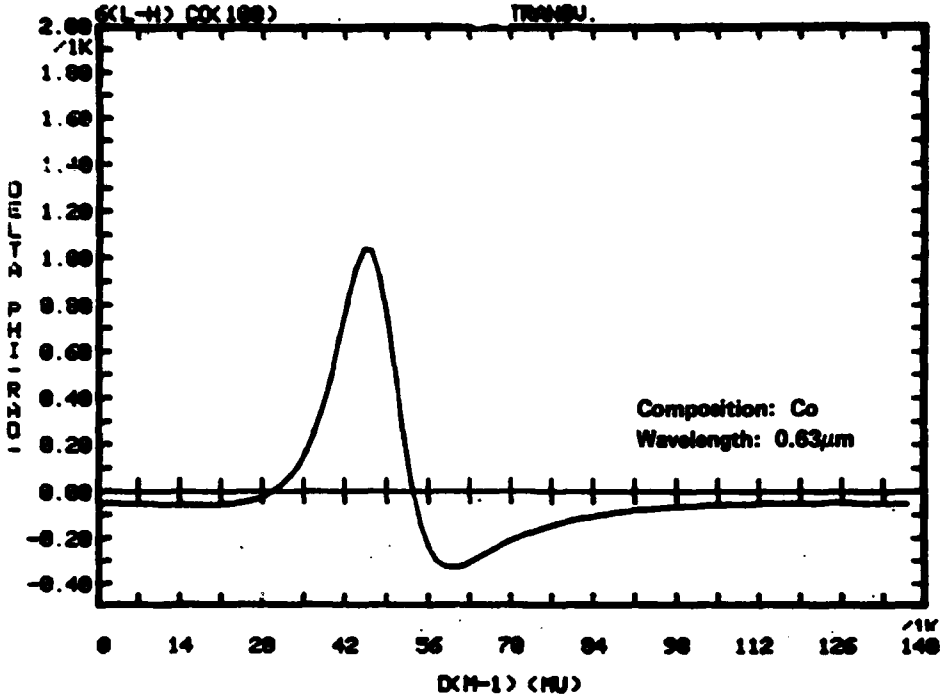

Fig. 11(c) — $\Delta\Phi$ vs tuning

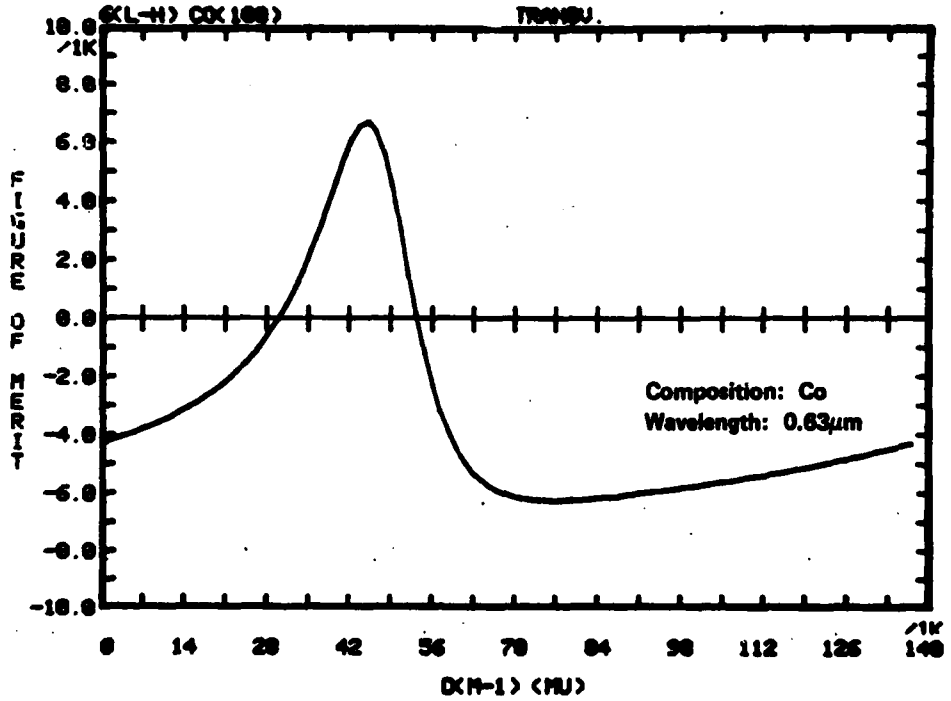

Fig. 11(d) — FM vs tuning

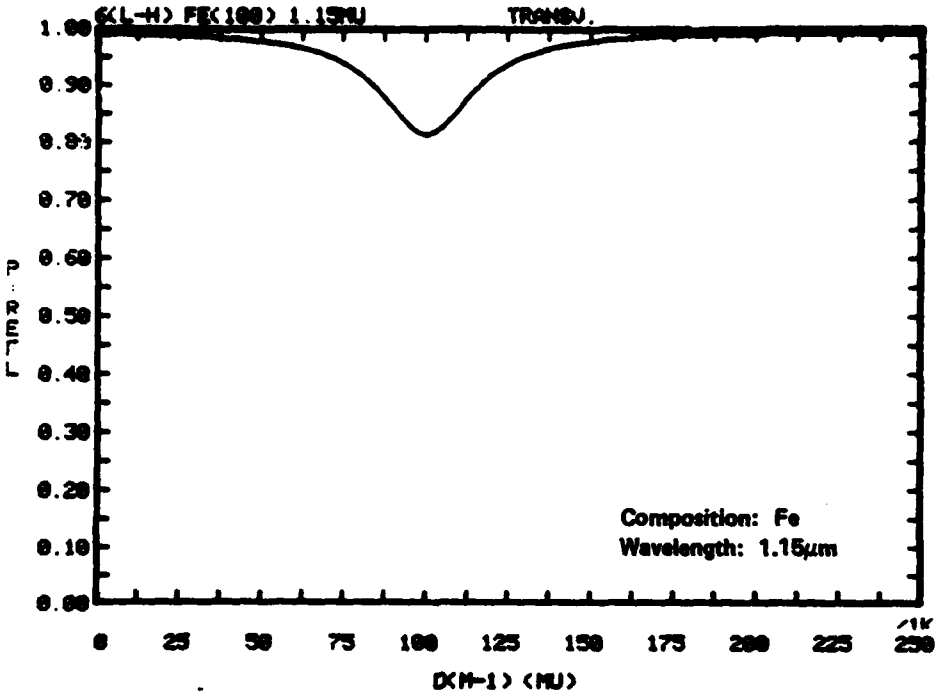

Fig. 12(a) — R vs tuning

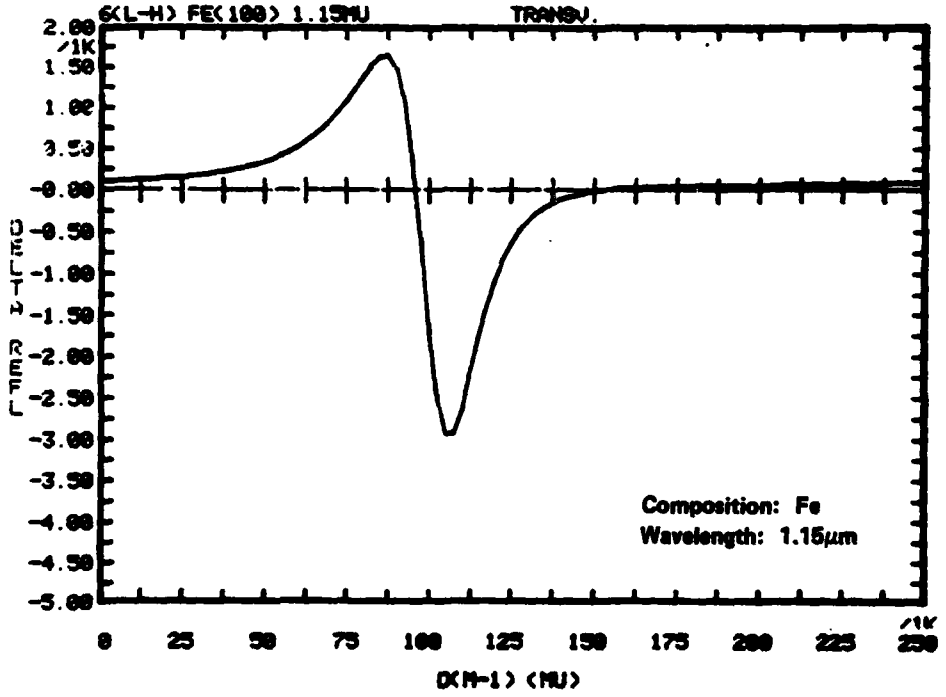

Fig. 12(b) — ΔR vs tuning

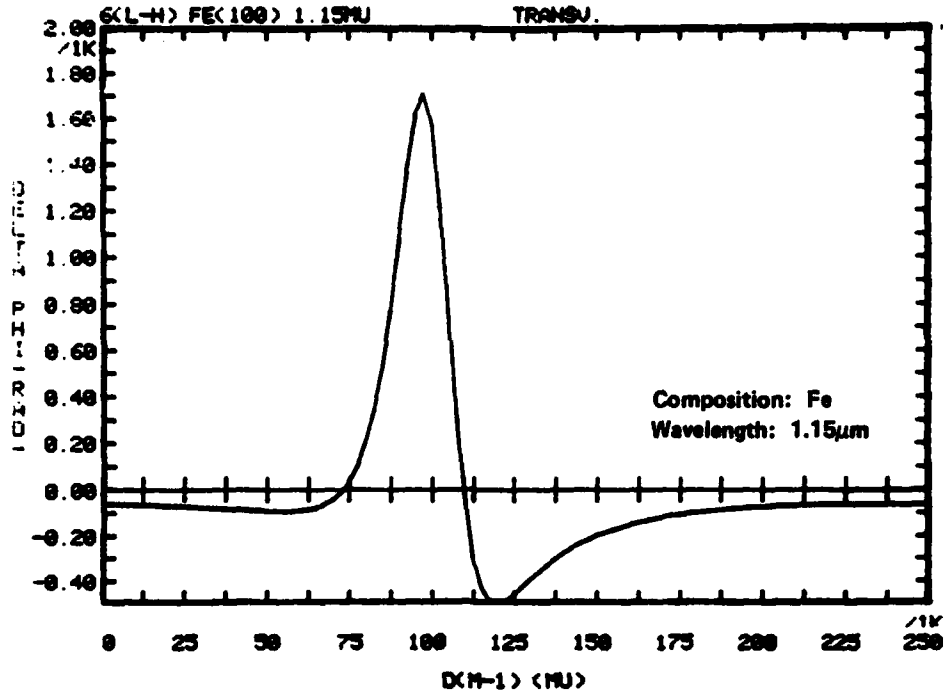

Fig. 12(c) — $\Delta\Phi$ vs tuning

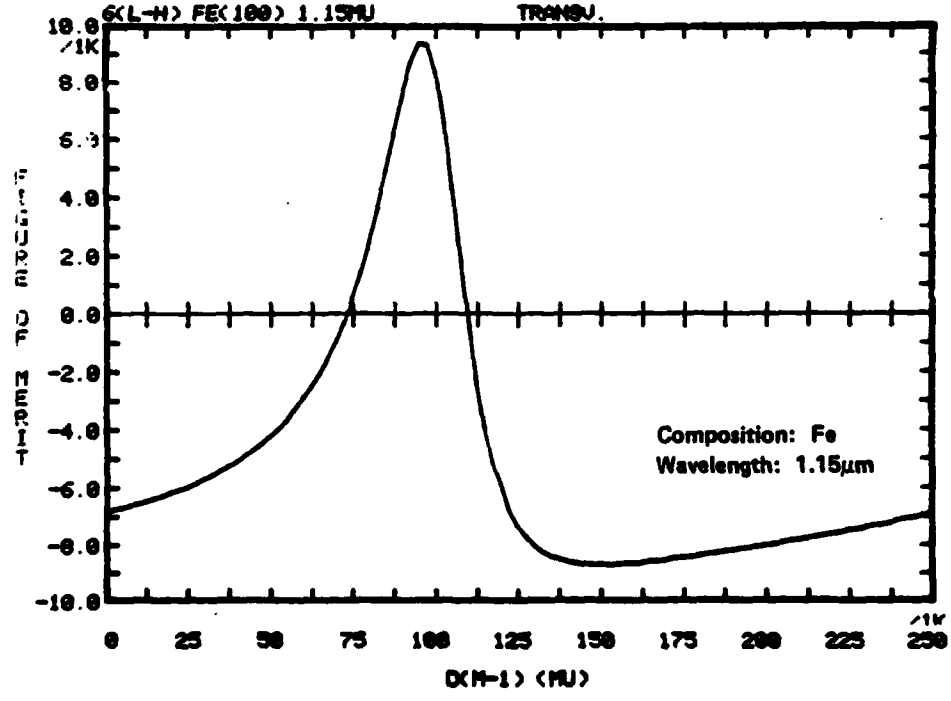

Fig. 12(d) — FM vs tuning

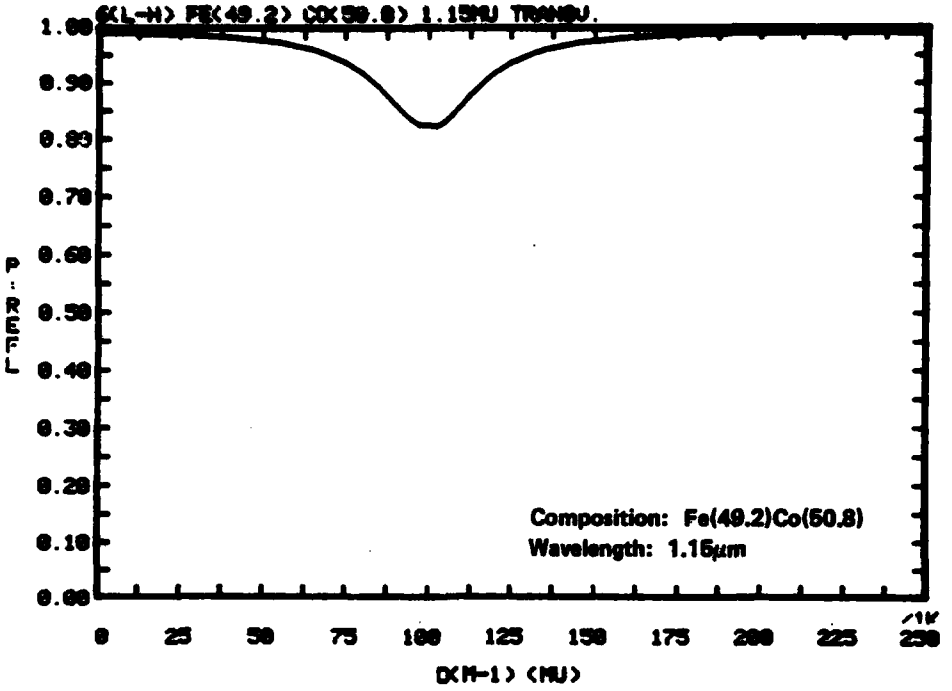

Fig. 13(a) — R vs tuning

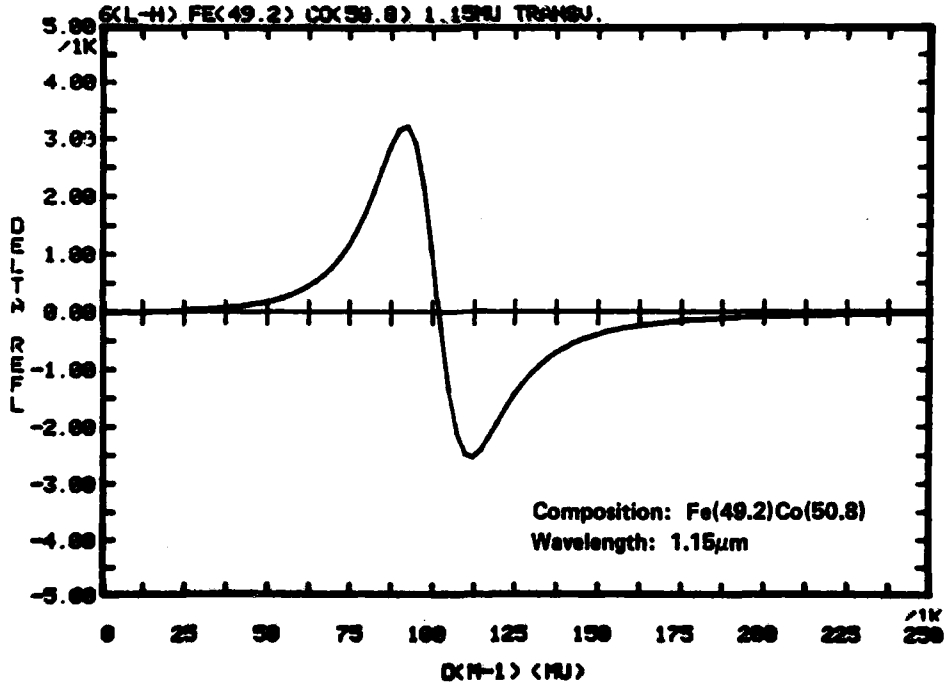

Fig. 13(b) — ΔR vs tuning

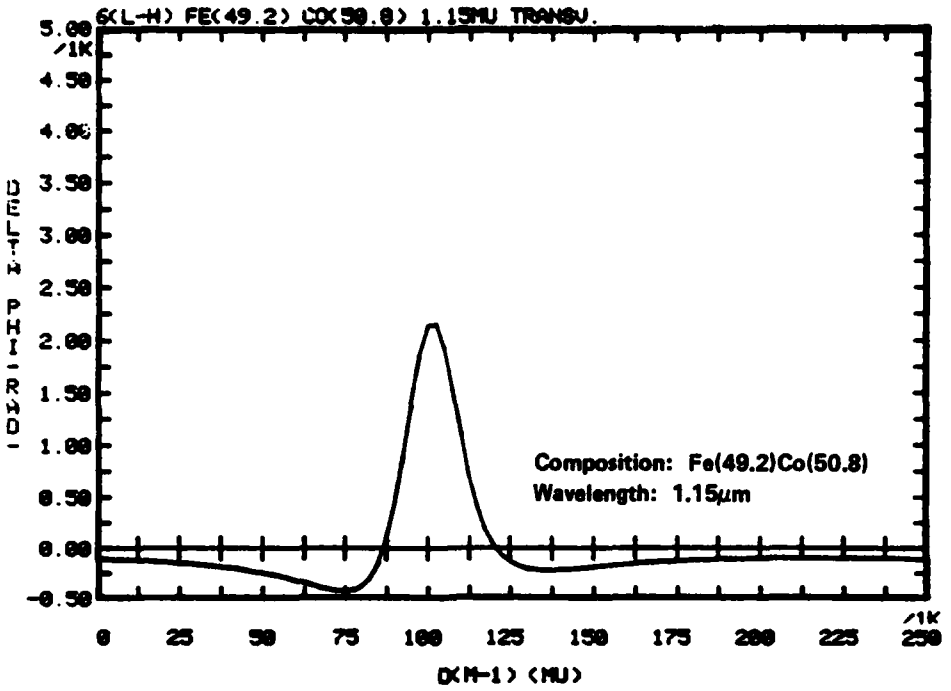

Fig. 13(c) — $\Delta\Phi$ vs tuning

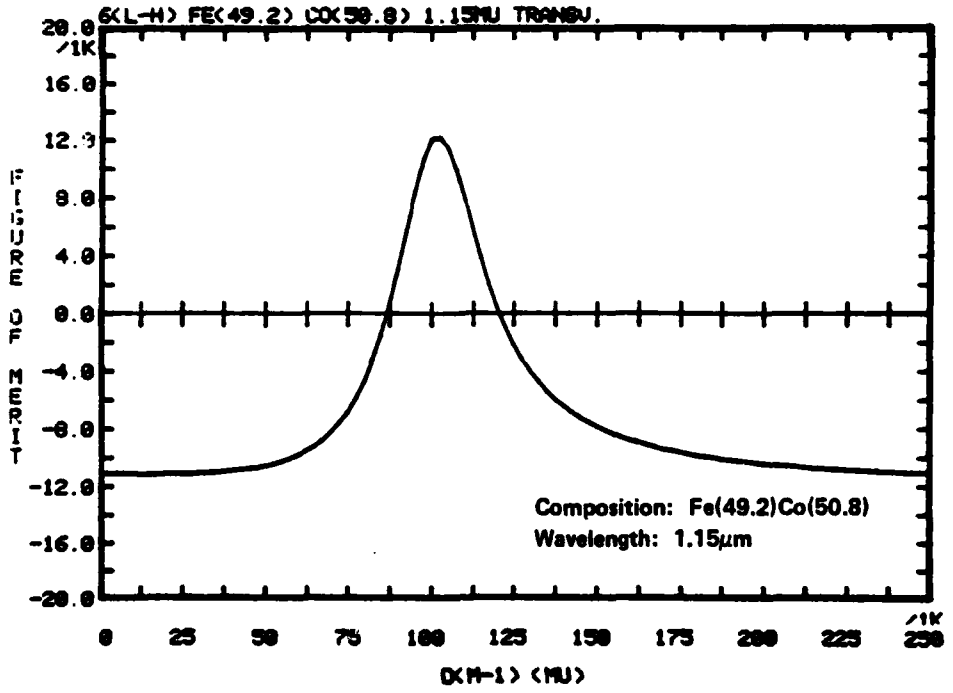

Fig. 13(d) — FM vs tuning

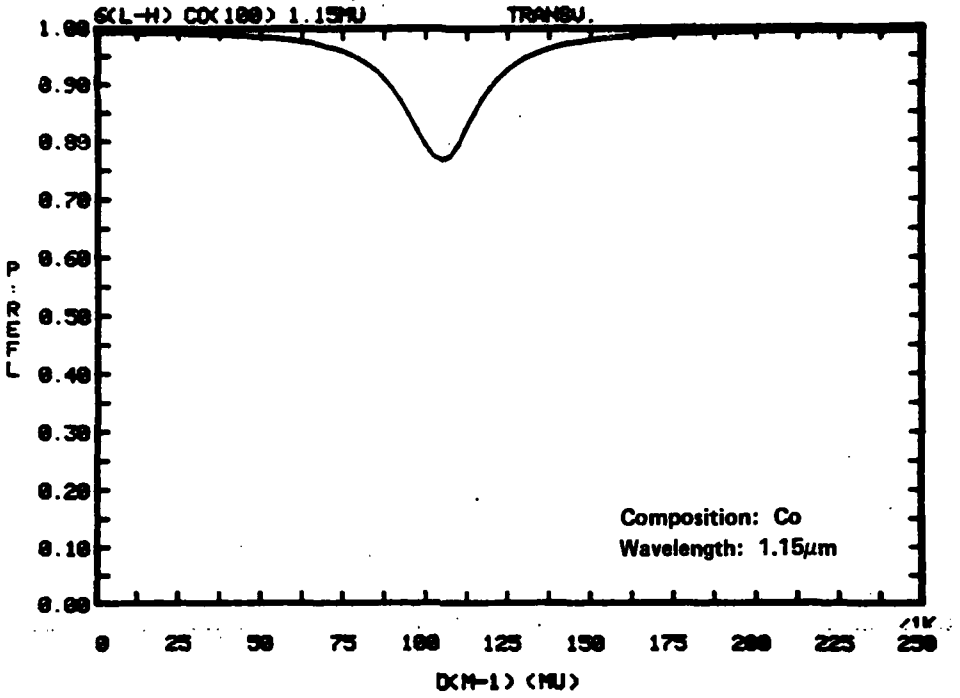

Fig. 14(a) — R vs tuning

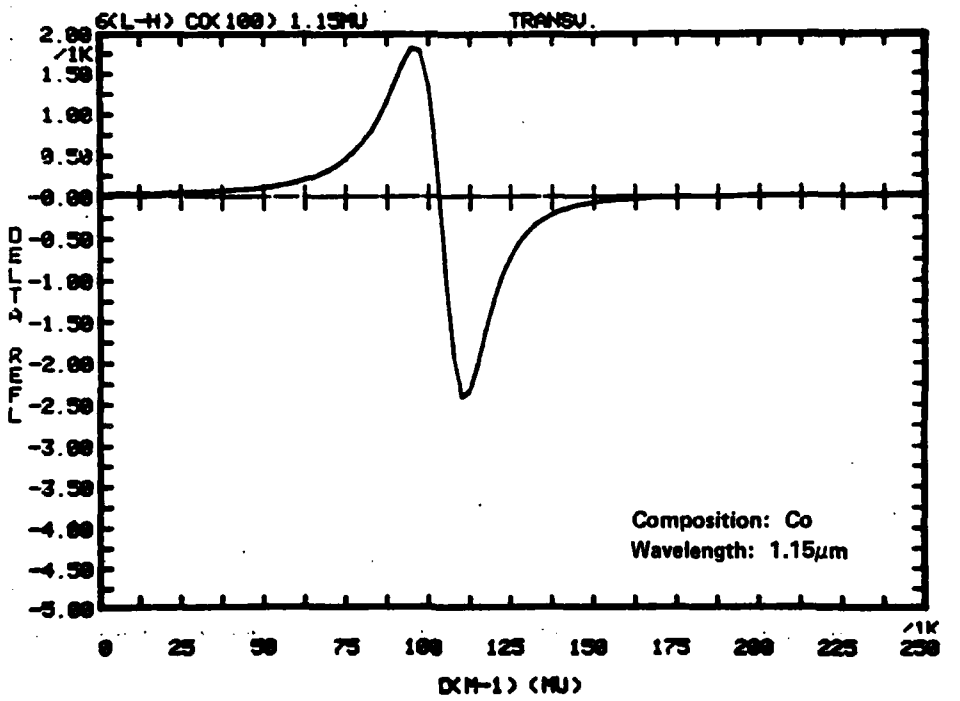

Fig. 14(b) — ΔR vs tuning

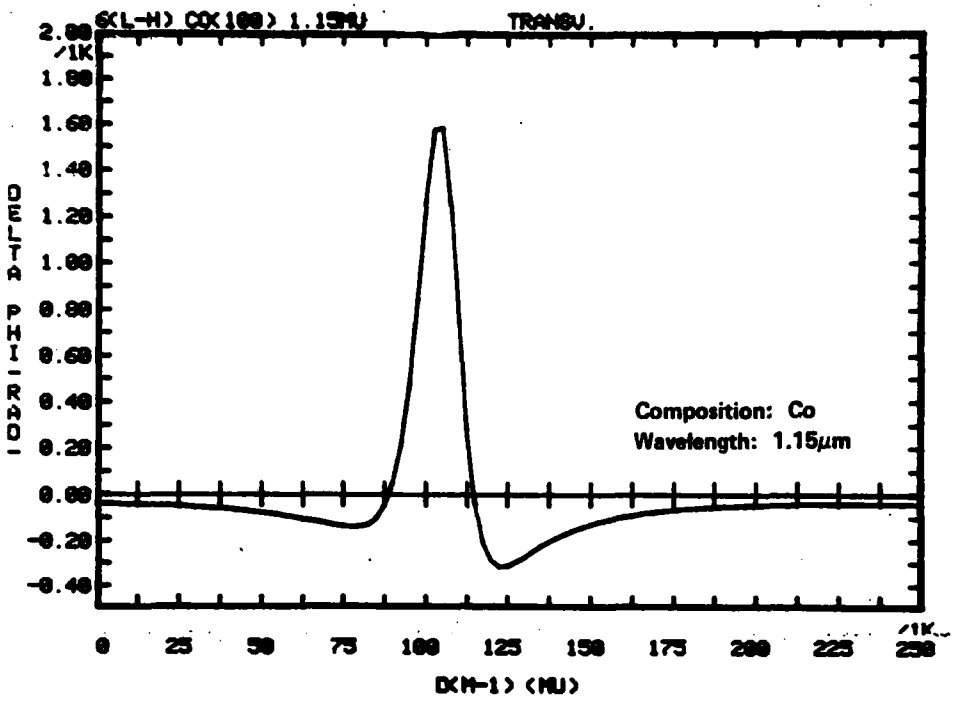

Fig. 14(c) — $\Delta\Phi$ vs tuning

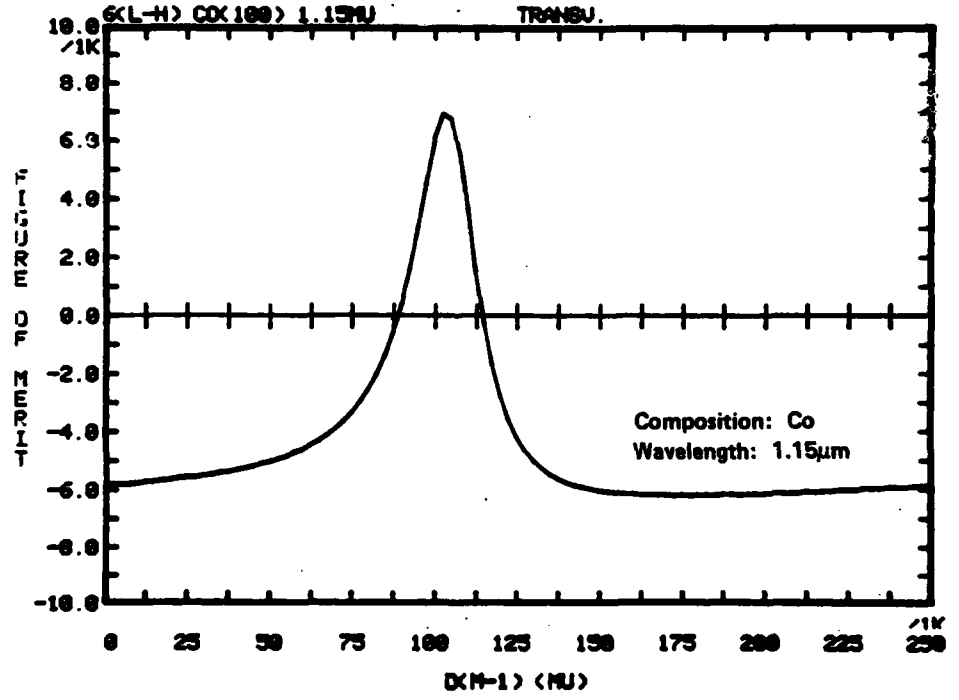

Fig. 14(d) — FM vs tuning

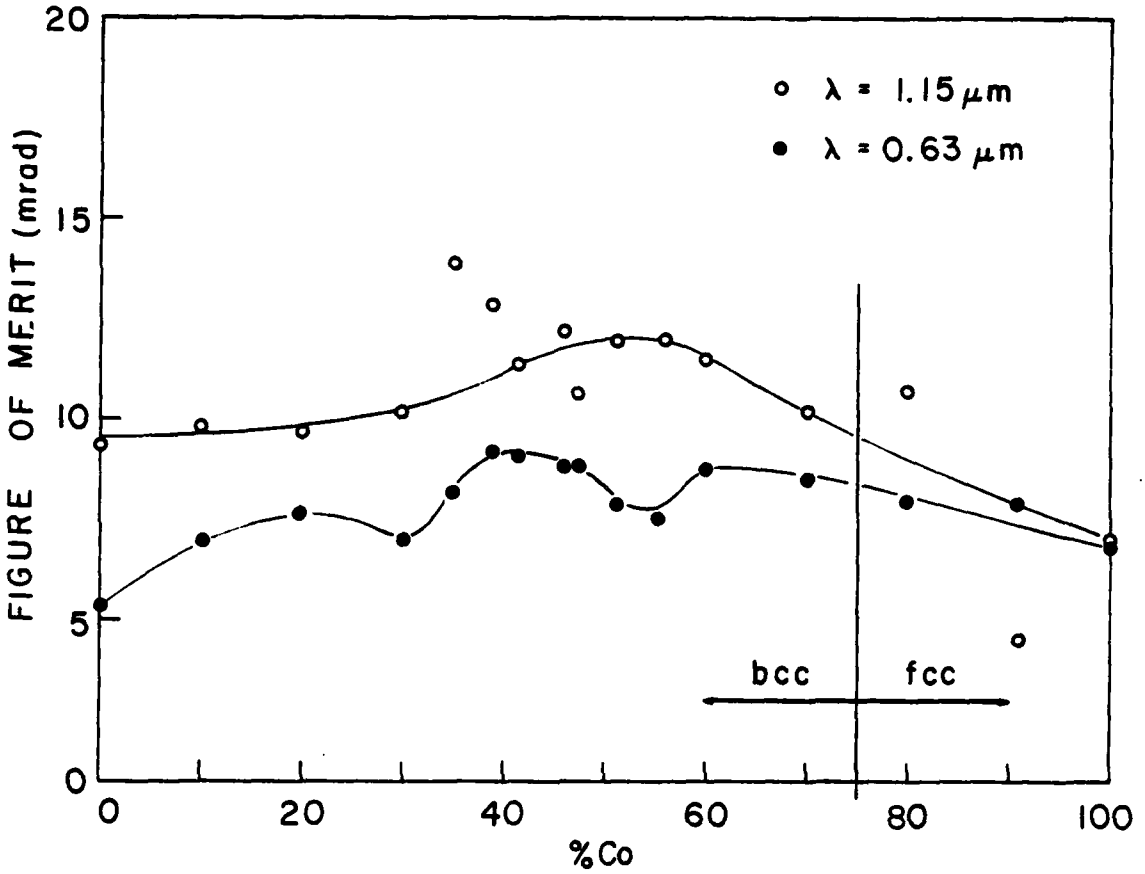

Fig. 15 — Peak figure of merit vs. composition for $\lambda = 0.63\mu m$ and $\lambda = 1.15\mu m$

References

[1] G.S. Krinchik and V.A. Artem'ev, Zh. Eksp. Teor. Fiz. 53, 1901-1912 (Dec. 1967).

[2] Yu.V. Kudryavtsev, I.V. Lezhnenko, and A.G. Lesnic, The 9th Inter. Coll. on Magnetic Films and Surfaces, Poznan, Poland (Aug. 1979).

[3] Jiro YAMASHITA, Shinya WAKOH, and Setzuro ASANO, J. Phys. Soc. Jap., 21, 53 (1966).

[4] C.C. Robinson, J. Opt. Soc. Amer. 54, 1220 (1964).

[5] J.A. Copeland, C.K. Kur, and E.J. Schneibner, Rev. Sci. Instrum. 36, 291 (1965).

[6] J.J. Krebs and W.G. Maisch, NRL Memorandum Report 4364, Sept. 1980.

[7] J.A. Oyedelè and M.F. Collins, Phys. Rev. B1, 16, 3208 (1977).

[8] D. Yoon and A. Bienenstock, Phys. Rev. 170, 631 (1968).

[9] M. Singh, C.S. Wang, and J. Callaway, Phys. Rev. B1, 11, 287 (1975).